Microtubule assembly in meiotic extract requires glycogen

Aaron C. Groen, Margaret Coughlin, and Timothy J. Mitchison
Department of Systems Biology, Harvard Medical School, Boston, MA 02115

ABSTRACT The assembly of microtubules during mitosis requires many identified components, such as γ-tubulin ring complex (γ-TuRC), components of the Ran pathway (e.g., TPX2, HuRP, and Rae1), and XMAP215/chTOG. However, it is far from clear how these factors function together or whether more factors exist. In this study, we used biochemistry to attempt to identify active microtubule nucleation protein complexes from *Xenopus* meiotic egg extracts. Unexpectedly, we found both microtubule assembly and bipolar spindle assembly required glycogen, which acted both as a crowding agent and as metabolic source glucose. By also reconstituting microtubule assembly in clarified extracts, we showed microtubule assembly does not require ribosomes, mitochondria, or membranes. Our clarified extracts will provide a powerful tool for activity-based biochemical fractionations for microtubule assembly.

INTRODUCTION

During mitosis, microtubule assembly is activated around chromatin through two pathways (Askjaer *et al.*, 2002; Gruss *et al.*, 2002; Kalab *et al.*, 2002; Tsai *et al.*, 2003; Sampath *et al.*, 2004; Kelly *et al.*, 2007; Maresca *et al.*, 2009). One pathway depends on Aurora B kinase as part of the chromosomal passenger complex (CPC; Vagnarelli and Earnshaw, 2004). The other depends on the small GTPase, Ran (Askjaer *et al.*, 2002; Gruss *et al.*, 2002; Kalab *et al.*, 2002; Tsai *et al.*, 2003; Maresca *et al.*, 2009). The Ran guanine nucleotide exchange factor (RanGEF), RCC1, binds to chromatin and locally activates Ran. RanGTP binds to importin β, which releases spindle assembly cargoes such as TPX2, NuMA, and HuRP from sequestration by importin α/β (Nachury *et al.*, 2001; Gruss *et al.*, 2002; Koffa *et al.*, 2006). This process, which is currently poorly defined, drives spindle assembly in the vicinity of chromatin (Carazo-Salas *et al.*, 1999).

A complete understanding of mitosis will arguably require reconstitution of mitotic spindle assembly and function from purified components. This is a huge undertaking and will likely proceed via reconstitution of subprocesses. Important progress has been made toward this goal, for example, in reconstitution of rapid dynamic instability (Kinoshita *et al.*, 2001), plus-tip tracking (Bieling *et al.*, 2007, 2008), and anaphase microtubule overlap zones (Bieling *et al.* 2010). However, important questions remain that hinder progress toward the larger goal. One of the primary questions is whether large particulate materials such as membranes or insoluble polymers are required for spindle assembly. There are hints in the literature that membranes and possibly some poorly defined "spindle matrix" are required for spindle assembly, but these potential biochemical requirements have not been definitively addressed (Chang *et al.*, 2004; Zheng and Tsai, 2006). In practical terms, one approach to answering these questions is to develop cell-free systems that support spindle assembly and to separate spindle assembly activities by fractionation.

Mitotic extracts from *Xenopus* eggs provide the most-used cell-free system for mitosis research (Sawin *et al.*, 1992; Desai *et al.*, 1999a). These are called "CSF extracts" in the literature; their high CDK1 activity and M-phase state are naturally stabilized by cytostatic factor (CSF; Moses and Masui, 1989, 1990). When supplemented with chromatin, they recapitulate assembly of the female meiosis-II spindle, which resides at the animal pole in unfertilized eggs, with considerable fidelity in terms of spindle size and shape (Desai *et al.*, 1999a). They are prepared by first packing eggs to remove buffer, and then gently crushing eggs by centrifugation (Desai *et al.*, 1999a). They are essentially undiluted cytoplasm, containing
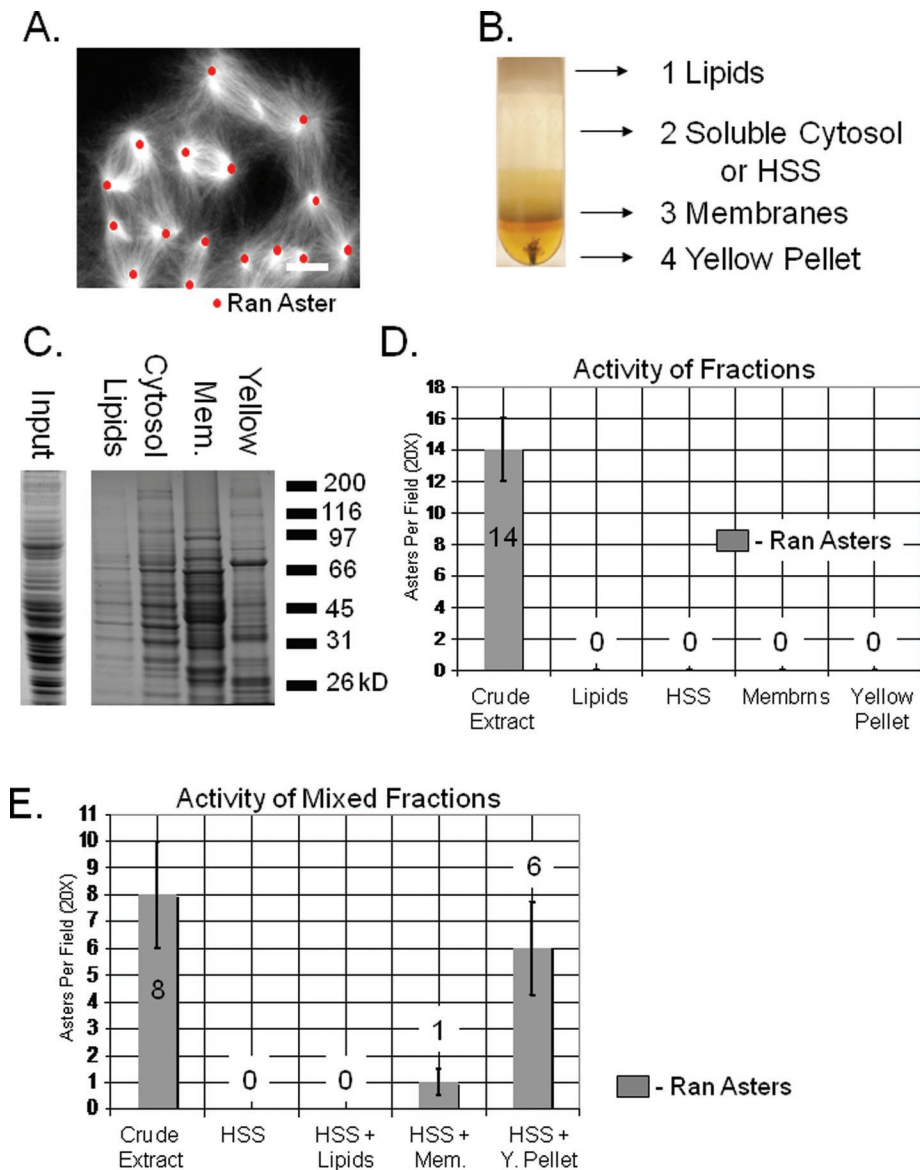
FIGURE 1: Microtubule assembly requires high-speed supernatant (HSS or cytosolic fraction) and particulate fractions. (A) The Ran-dependent microtubule-assembly assay used to quantify microtubule assembly. A 20× magnified field view of 16 asters (16 APF) after Ran(Q69L)GTP (1 mg/ml) addition to crude *Xenopus* extracts supplemented with X-rhodamine tubulin (50 μg/ml). Scale bar: 5 μm. (B) The four layers separated after high-speed centrifugation of 5 ml of crude *Xenopus* meiotic extract: (1) lipids, (2) soluble cytosol (or HSS), (3) membranes, and (4) yellow pellet. (C) Coomassie Blue–stained gel of fractions (1–4) presented in B. Input is crude *Xenopus* meiotic egg extracts (100 μg sample per lane). (D) Ran-dependent microtubule-assembly assay of each isolated fraction presented in B. The average number of microtubule asters per 20 fields after addition of 1 mg/ml of Ran(Q69L)GTP to crude extract (input) and each of the isolated fractions presented in B. None of the separated fractions contain microtubule-assembly (or aster) activity. Error bars = SD, n = 8. (E) Ran-dependent microtubule-assembly assay after mixing fraction presented in B. The average number of microtubule asters per 20 fields after addition of 1 mg/ml of Ran(Q69L)GTP to crude extract (input), soluble cytosol (HSS), and combinations of HSS plus lipids, HSS plus membranes, and HSS plus yellow pellet. Note the bulk of the activity returned in HSS plus yellow pellet combination. Error bars = SD, n = 7.

tional sense. It has long been known these extracts, when clarified by centrifugation to remove membrane and ribosomes, no longer support spindle assembly (T. Mitchison, unpublished data) or even normal microtubule dynamics (Desai *et al.*, 1997; Parsons and Salmon, 1997). It has been unclear why this is the case—does centrifugation remove some important particulate component required for spindle assembly, or does it merely damage the extract in some way, for example, by altering the activity of the kinase-phosphatase system that regulates cell cycle state? Here we address this question for one important aspect of spindle assembly, microtubule polymerization stimulated by RanGTP, using activity-based biochemical fractionation, and we develop methods for clarifying *Xenopus* egg extract while maintaining the mitotic state.

RESULTS

Ran-dependent microtubule assembly requires cytosol and particulate fractions

RanQ69L, which is defective in GTP hydrolysis (Bischoff *et al.*, 1994; Klebe *et al.*, 1995), promotes abundant microtubule assembly in crude CSF extract within 30 min (Figure 1A; Wilde *et al.*, 2001). In mitotic extracts, microtubules typically aggregate into asters under the influence of dynein once they are assembled (Buendia *et al.*, 1990; Verde *et al.*, 1991). We quantified assembly by counting the number of asters per microscope field (reference dots in Figure 1A), which was easy using relatively low magnification imaging.

To test for a particulate requirement in microtubule assembly promoted by RanQ69L, we clarified the extract by high-speed centrifugation (90 min at 200,000 × *g*). To stabilize high CDK1 levels in egg extract during centrifugation and dilution, we supplemented it with nondegradable cyclin B (Δ90) and 50 mM sucrose (Murray and Kirschner, 1989; Murray *et al.*, 1989). If either of these were omitted, our results were irreproducible. With them, we were always able to prepare a clarified preparation that retained its mitotic state as judged by assembly of asters with 10 μM Taxol or 10% dimethyl sulfoxide (DMSO) and confirmed by Western blots of extracts probed with the mitosis-specific phosphoprotein antibody, MPM-2 (Supplemental Figure 1A; Davis *et al.*, 1983). Centrifugation separated the crude extract into four distinct layers: lipids, soluble cytosolic proteins, membranes, and a yellow pellet (Figure 1B–C). Each fraction was assayed for microtubule assembly. To do this, we washed and resuspended the fractions containing particulates (lipids, membranes, and yellow pellet fractions) in a physiological salt buffer

abundant organelles, ribosomes, and other particulates. They support vigorous energy metabolism, making and hydrolyzing ~1 mM ATP/min, by either respiration or anaerobic glycolysis (Niethammer *et al.*, 2008). However, dilution with buffer or passage over chromatography columns changes their properties and activities greatly. Thus they are not a tractable biochemical system in the conven-

(CSF-XB equal to the starting volume; see *Materials and Methods*) and assayed the fractions by addition of RanQ69L and X-rhodamine tubulin (10 μg/ml; Figure 1D). The number of asters was quantified over 20 different fields per coverslip (see *Materials and Methods*).

The soluble cytosolic layer, which we will also refer to as the high-speed supernatant (HSS), contained all the previously identified factors necessary for microtubule assembly in this system, including XMAP215, TPX2, γ-tubulin, and HuRP (Figure 1C; unpublished data; Wittmann *et al.*, 2000; Popov *et al.*, 2001; Casanova *et al.*, 2008; Groen *et al.*, 2009). Surprisingly, we could not detect Ran-dependent microtubule-assembly activity in this layer (0 asters per field [APF]; Figure 1D). Also, none of the particulate fractions was individually active.

We next tested whether mixing different fractions separated during high-speed centrifugation reconstituted Ran-dependent microtubule assembly. Briefly, each fraction (lipids, membranes, and yellow pellet) was resuspended and pelleted four times: the first three times with CSF-XB (to wash) and the last time with HSS (to minimize dilution). Finally, the samples were resuspended in HSS (equal to original volume of the isolated crude extract; see *Materials and Methods*) and assayed for Ran-dependent microtubule assembly. In the mixing experiments, both the membrane fraction (1 APF) and the yellow pellet (8 APF; Figure 1E) rescued microtubule assembly when added back to HSS. Rescue activity was most concentrated in the yellow pellet and similar to activity in crude extract; asters assembled 30 min after Ran addition. Thus the yellow pellet contained the bulk of the rescue activity for Ran-promoted microtubule assembly in HSS.

Glycogen is required for Ran-dependent microtubule assembly

We next determined what factor(s) from the yellow pellet were required to restore Ran-promoted microtubule assembly when added to HSS. SDS–PAGE and Coomassie Blue staining indicated numerous proteins were present in this fraction (Figure 1C). To test for the dependence of activity on proteins, we pelleted and resuspended the yellow pellet two times with CSF-XB, and either boiled it for 5 min or extracted it with phenol-chloroform (using the aqueous layer). The treated samples were next pelleted and resuspended three times: twice with CSF-XB (to wash) and once in HSS (to minimize dilution). Finally, as previously, the samples were resuspended in HSS (equal to original volume of the isolated crude extract). Microtubule-assembly activity was retained after boiling and in the aqueous phase of phenol-chloroform extraction (6 APF; unpublished data; Figure 2A). To test for a membrane requirement, the yellow pellet was washed (as described previously for phenol-chloroform assays) with CSF-XB containing 10% Triton-X. Activity was retained after Triton-X treatment (7 APF; Figure 2A), suggesting there was no membrane requirement contained in the yellow pellet. We also found that RNase treatment had no effect on activity (7 APF; Figure 2A). These data suggested proteins, membrane-bound organelles, or RNA/ribosomes were not involved.

Previous reports showed that the yellow pellet contained large amounts of glycogen (Hartl *et al.*, 1994). Through phenol-chloroform extraction and precipitation by ethanol, we estimate that crude *Xenopus* egg extract contains approximately 26 mg/ml of glycogen. We found that when the yellow pellet was digested with α-amylase prior to mixing with HSS, microtubule assembly was inhibited (0 APF; Figure 2A). Thus either glycogen or an unidentified factor eluting upon glycogen breakdown stimulates microtubule assembly in HSS containing RanQ69L.

To determine whether glycogen was sufficient to reconstitute microtubule assembly, we titrated purified bovine glycogen in HSS

and added Ran (Figure 2B). The commercial glycogen, which we further washed in CSF-XB, contained no detectable proteins or RNA. Addition of purified bovine glycogen to HSS caused a concentration-dependent increase in microtubule aster assembly in the presence of RanQ69L (Figure 2, B–C). Glycogen concentrations of 200 mg/ml induced microtubule assembly even when RanQ69L was omitted (Figure 2C), as shown by Western blots of the microtubule pellets with or without Ran in HSS.

The addition of Ran to crude extracts induces both aster-like and bipolar spindle-like structures (Tsai *et al.*, 2003). We noticed that the percentage of bipolar microtubule structures increased with higher concentrations of glycogen up to 100 mg/ml. For example, for 5 mg/ml of glycogen, all structures appeared to be symmetrical asters (Figure 2, B and D), while with 20 mg/ml of glycogen, ~33% of the structures were bipolar, and 66% of the structures were bipolar with 100 mg/ml (Figure 2, B and D). Thus glycogen may also induce bipolarity of microtubule structures, most likely by providing enhanced microtubule assembly.

Membrane and ion requirements

Although the HSS used above is free of ribosomes, it still contains some membranes, presumably because the high protein concentration makes the HSS sufficiently dense that light membranes and some residual glycogen do not sediment reliably. To completely remove membranes/glycogen from our extracts, we first diluted the crude extract 10-fold, then centrifuged. The resulting highly clarified, but diluted, HSS was concentrated using a centrifugal filtration unit with a 10-kDa cutoff membrane (Figure 3B; see *Materials and Methods*). The clarified extract did not contain visible membranes when viewed with the lipophilic membrane dye, FM4-64 (Figure 3A; Bolte *et al.*, 2004). We called this fully clarified, reconcentrated preparation C-HSS.

The buffer used for dilution turned out to be extremely important. After testing many conditions, we found that inclusion of 5–10 mM P_i (in the form of potassium phosphate) into a physiological salt buffer (pH range of 7.2–7.8) was required for Ran-promoted microtubule assembly in C-HSS supplemented with glycogen (Figure 3C; see Table 1; unpublished data). When viewed with electron microscopy, Ran asters assembled in C-HSS were free of the

Condition[a]	Activity units (APF)
HEPES: 10 mM, pH 7.7	0
HEPES: 10 mM, pH 7.2	0
Citrate: 10 mM, pH 7.7	0
Tris: 10 mM, pH 7.7	0
Histidine: 10 mM, pH 7.7	0
Serine: 10 mM, pH 7.2	0
Phosphate: 10 mM, pH 7.2	7
HEPES/phosphate: pH 7.7	6
4X-concentrated[b]	0
4X-concentrated[b] plus glucose-6-phosphate	9

[a] Each condition also included the following: 100 mM KCl, 5 mM EGTA, 1 mM MgCl₂, 1 mM ATP, 1 mM GTP, 1 mM DTT, 1 mM creatine phosphate.
[b] The following dilution buffers were used: 10 mM potassium phosphate, pH 7.2, 100 mM KCl, 5 mM EGTA, 1 mM MgCl₂, 1 mM ATP, 1 mM GTP, 1 mM DTT, 5 mM glucose-6-phosphate, 1 mM creatine phosphate.

TABLE 1: C-HSS dilution buffers.

A. Yellow Pellet Treatments

B. Glycogen Titration in HSS
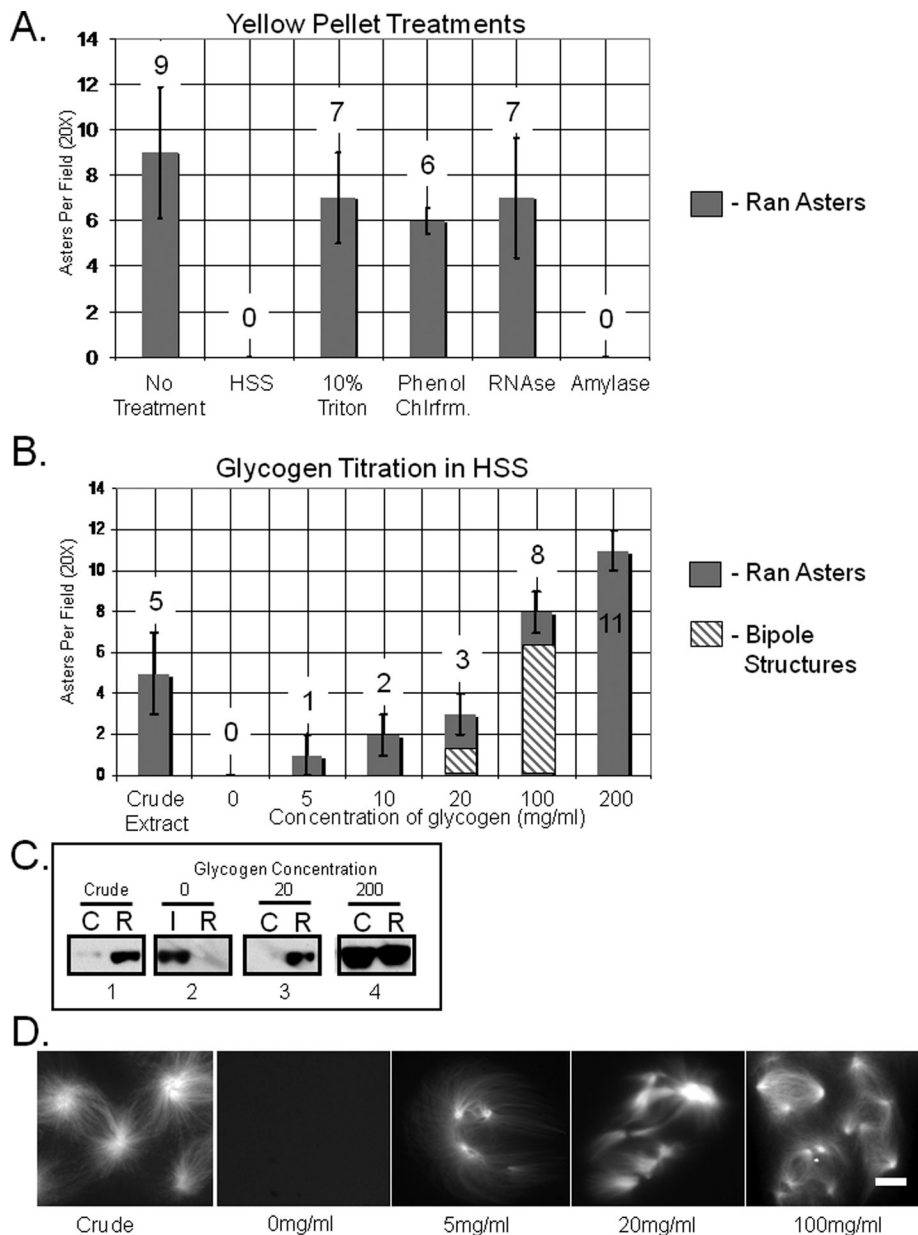
C.

D.

FIGURE 2: Glycogen is required for microtubule assembly. (A) Ran-dependent microtubule activity assays of yellow pellet after various treatments. Activity is amylase-sensitive. The average number of microtubule asters per 20× magnified field after addition of 1 mg/ml of Ran(Q69L)GTP to HSS plus yellow pellet (positive control), HSS (negative control), or HSS plus yellow pellet after treatment with: 10% Triton (Triton), phenol-chloroform extraction (phenol chlrfrm), RNase, or amylase. Error bars = SD, n = 4. (B) Ran-dependent microtubule assays with glycogen titration in HSS. Purified bovine glycogen restores Ran-dependent microtubule assembly to HSS and is titratable. The average number of microtubule asters per 20× magnified field after addition of 1 mg/ml of Ran(Q69L)GTP to crude extract (positive control), HSS (negative control) with no additional glycogen (0), and HSS plus purified bovine glycogen (5, 10, 20, 100, and 200 mg/ml). Higher concentrations of glycogen (20 and 100 mg/ml) increase bipolarity of structures (10 mg/ml = 0% bipolar structures, 20 mg/ml = 33% bipolar structures, and 100 mg/ml = 66% bipolar structures). Error bars = SD, n = 4. (C) Glycogen restores microtubule assembly to HSS. Microtubule pelleting assay: (1) Pellets of crude extract plus (R, Ran) and minus (C, control) Ran(Q69L)GTP, (2) HSS input (I), pellet of HSS plus Ran(Q69L)GTP (R), (3) pellet of HSS plus 20 mg/ml glycogen plus (R) and minus (C, control) Ran(Q69L)GTP, (4) pellet of HSS plus 200 mg/ml glycogen plus (R) and minus (C, control) Ran(Q69L)GTP. Note 200 mg/ml of glycogen induces ectopic microtubule assembly without Ran. (D) Representative images of microtubule structures assembled in Ran(Q69L)GTP-treated crude extracts (control) and Ran(Q69L)GTP-treated HSS plus 0, 5, 20, or 100 mg/ml glycogen. Note presence of more bipolar structures at 100 mg/ml of glycogen. Scale bar: 3 μm.

electron-dense material we observed on asters assembled in crude extract (Figure 3D). Crude extract asters contained many membranes and ~25-nm electron-dense particles, most likely corresponding to mitochondria, endoplasmic reticulum (ER), ribosomes, and other structures (Figure 3D). Glycogen restored microtubule assembly in C-HSS treated with up to 1% Triton-X (Figure 3E). We noticed the asters were smaller at 0.1–0.5% Triton-X (1 μm compared with 3 μm in length; Figure 3E), while the asters were smaller and aggregated at 1% Triton-X (Figure 3E). Thus either Triton-X is disrupting protein interactions/tubulin dynamics or normal aster structure requires membranes that are not removed by our purification. Collectively, our data suggest Ran-dependent microtubule assembly does not require membranes or membrane organelles. It does require glycogen and relatively high concentrations of phosphate. The rest of the assays presented in this study used C-HSS made with 10 mM P_i and glucose-6-phosphate unless otherwise stated.

Glycogen provides both crowding and metabolic roles

We considered two main hypotheses for glycogen activity, as a nonmetabolically active crowding agent or as a metabolic source of glucose. Other activities, such as acting as a scaffold for phosphatases, have been considered in the literature (Hartl *et al.*, 1994; Lourim and Krohne, 1998). Dextran (a glucose polymer that is not an amylase substrate) and methyl-cellulose are nonmetabolizable and are traditionally used as crowding agents (Zimmerman and Minton, 1993). Addition of either methyl-cellulose or dextran (at concentrations comparable to the endogenous glycogen concentration) did not reproducibly restore Ran-dependent microtubule assembly to C-HSS (Figure 4A), suggesting a crowding agent alone is not sufficient.

We next considered the metabolic activity of glycogen. Glycogen is catabolized into glucose-1-phosphate, which is quickly converted into glucose-6-phosphate, the metabolite ultimately used metabolically (Roach, 2002). We added thio-NADP as a rapid test of glucose metabolism in C-HSS. Reduction of this compound to thio-NADPH is irreversible, depends on glucose metabolism (via glucose-6-phosphate dehydrogenase), and is readily observed by measuring its absorbance at 405 nm (Seimiya *et al.*, 2004). C-HSS did not generate a 405-nm absorbance, while C-HSS plus glycogen did. C-HSS plus dextran or methyl-cellulose did not generate 405-nm absorbance when
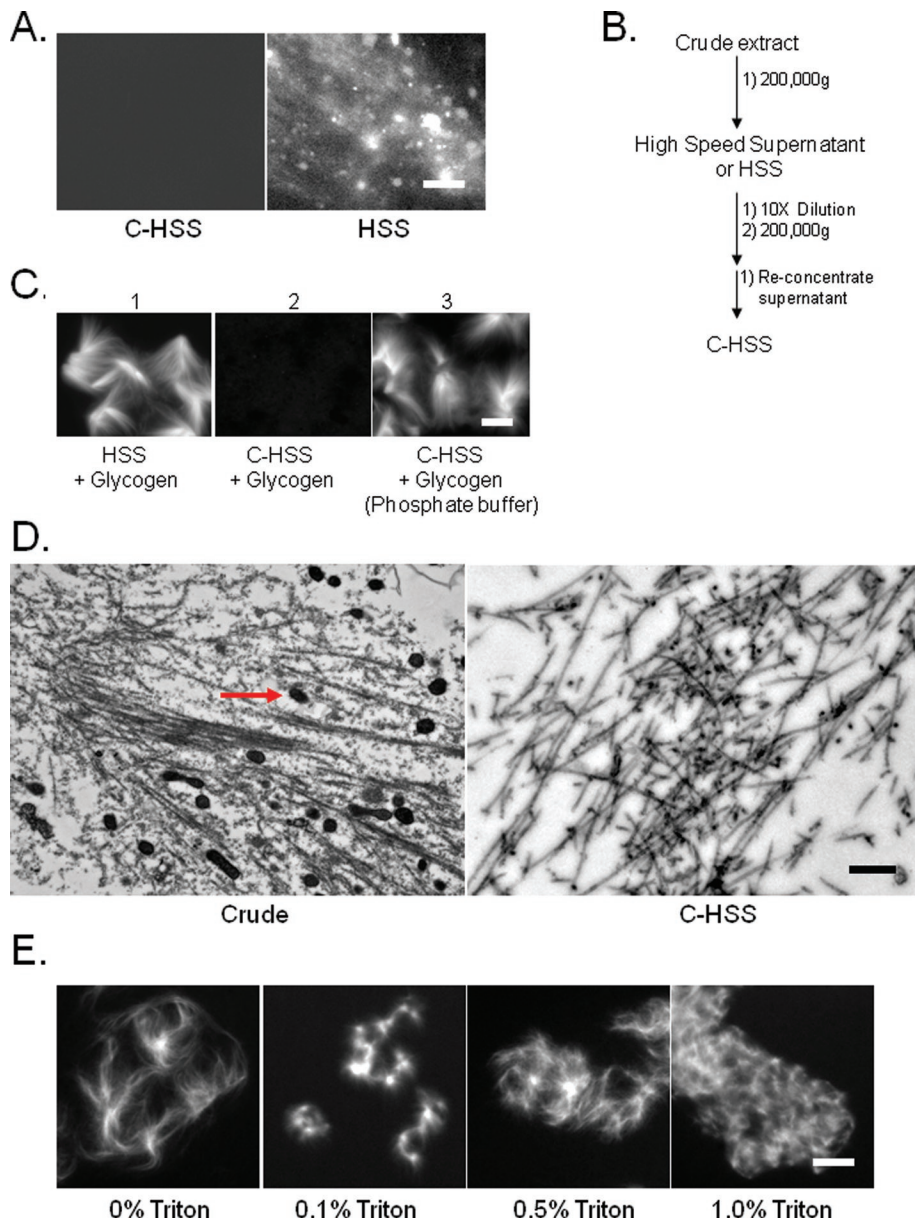
FIGURE 3: Membranes are not required for microtubule assembly. (A) FM4-64 staining of membrane structures present in C-HSS (left) and HSS (right). Scale bar: 1 μm. (B) Purification scheme of C-HSS. (C) C-HSS requires phosphate in dilution buffer for glycogen to restore microtubule assembly. Ran-dependent microtubule assembly in (1) HSS plus glycogen (30 mg/ml), (2) C-HSS diluted without a phosphate buffer (S-CSF-XB) plus glycogen (30 mg/ml), and (3) C-HSS diluted with a phosphate buffer (S-CSF-XB-phosphate) plus glycogen (30 mg/ml). Scale bar: 5 μm. (D) Electron micrograph of Ran-induced microtubules in crude extract (left) or C-HSS (right) supplemented with glycogen (30 mg/ml). Note the electron-dense mitochondria (red arrow) in crude extracts. Also, microtubules appear to bind more electron-dense material than asters assembled in C-HSS (right). Scale bar: 500 nm. (E) Ran-induced microtubules assemble in 0% (control), 0.1%, 0.5%, and 1% Triton-X–treated C-HSS supplemented with glycogen (30 mg/ml). Scale bar: 3 μm

drial enzyme and C-HSS is devoid of mitochondria (unpublished data; Golshani-Hebroni and Bessman, 1997). Glucose-6-phosphate did not restore microtubule assembly (unpublished data), suggesting glucose metabolism alone is not sufficient to restore microtubule assembly.

Addition of glucose-6-phosphate (5 mM) and either dextran or methyl-cellulose (~20 mg/ml) completely restored Ran-dependent microtubule assembly in C-HSS (6 APF; Figure 4, A and C; unpublished data). The data suggest glycogen plays both a metabolic and a crowding role. They also argue against a more exotic role of glycogen, such as acting as a phosphatase scaffold.

Crowding agents can be viewed as acting by increasing the concentration of macromolecules. To test whether this could account for the nonmetabolic action of glycogen in our system, we concentrated C-HSS two- (2X), three- (3X), or fourfold (4X) by centrifugation onto a 10-kDa cutoff membrane. 1X-C-HSS is defined as the protein concentration present when C-HSS is reduced in volume back to the volume of the extract from which it originated. 1X-C-HSS ranged from 30–40 mg/ml protein using Bradford protein assay with bovine serum albumin (BSA) as the protein standard, while crude extract was more than 100 mg/ml (Figure 4B). When C-HSS was concentrated to 3X or 4X and supplemented with glucose-6-phosphate, microtubule assembly was restored to the same extent as in crude extract (6–9 APF for each condition; Figure 4, B and D). This activity required addition of glucose-6-phosphate, implying concentration can replace the crowding activity of glycogen, but not its metabolic activity. 2X-C-HSS was competent to assemble microtubules, although not to the same extent as crude extract (9 APF for crude extract, 2 APF for 2X-C-HSS; Figure 4, B and D). Similar to when higher concentrations of glycogen were added to C-HSS (100 mg/ml; Figure 5D), the more highly concentrated C-HSS (4X compared with 3X) assembled more bipolar structures (Figure 4D).

Which microtubule-assembly factors were most sensitive to dilution? The concentrations of tubulin, TPX2, and XMAP215—all factors required for microtubule assembly—varied to the same extent in each fractionated extract (Figure 4E2). However, HSS actually had higher concentrations (greater than one-third more) of each factor compared with crude extract (Figure 4E2), suggesting dilution of tubulin, TPX2, or XMAP215 did not cause loss of Ran-dependent microtubule assembly in HSS. C-HSS contained approximately one-half the concentrations of each factor, compared with crude extract (Figure 4E2). However, when C-HSS was concentrated 2X (2X-C-HSS), Ran-dependent microtubule assembly was not restored to

thio-NADP was added, showing dextran and methyl-cellulose are not catabolized, as expected (Supplemental Figure 2A). Thus C-HSS does not have an available metabolic source of glucose for energy production and reducing equivalents.

Addition of glucose-6-phosphate (1–10 mM) to C-HSS enabled the reduction of thio-NADP, suggesting restoration of metabolic activity (unpublished data). We did not add glucose, because hexokinase, the enzyme producing glucose-6-phosphate, is a mitochon-
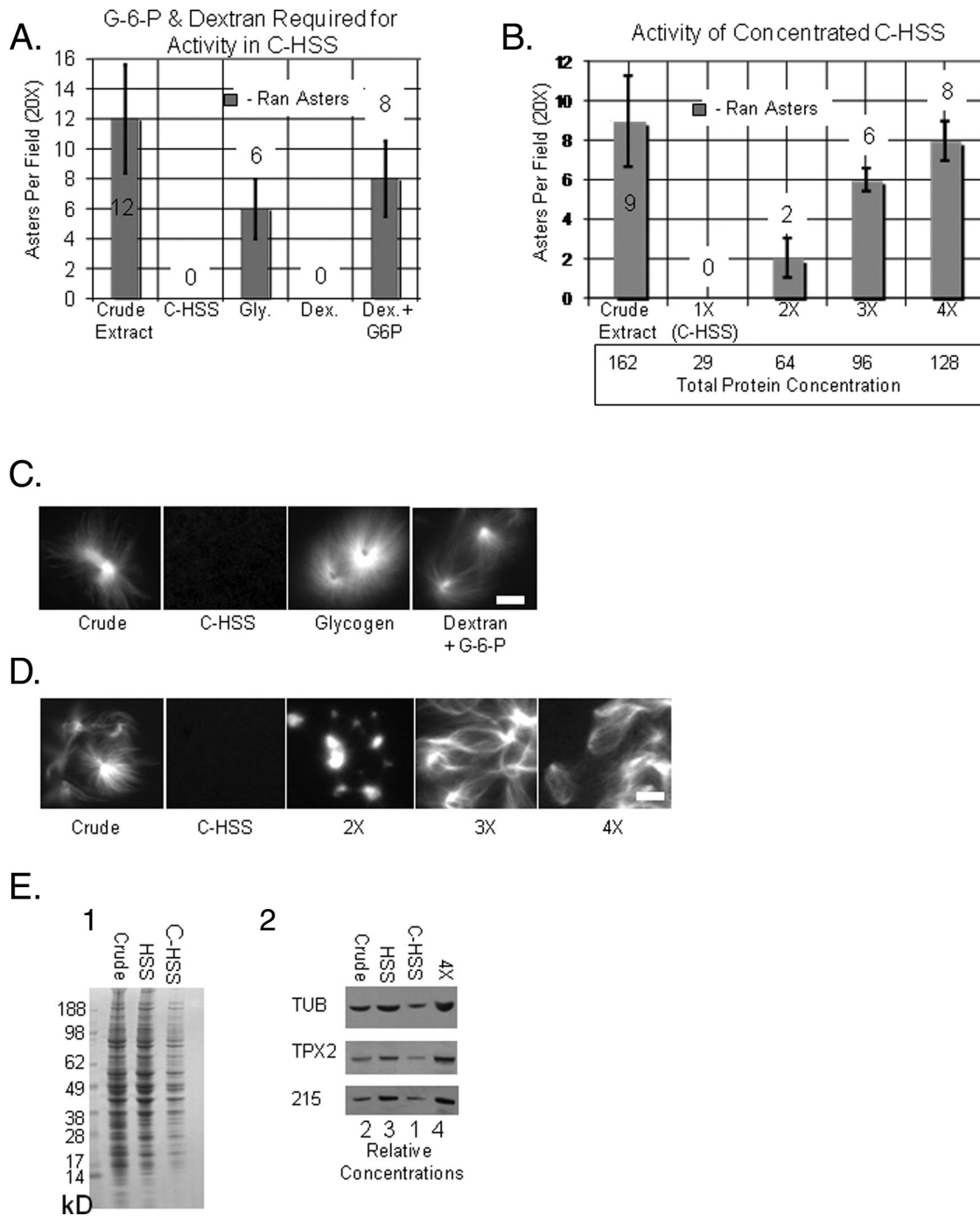
FIGURE 4: Glycogen acts as a molecular crowding agent and metabolic source of glucose. (A) Ran-dependent microtubule-assembly assay showing glucose-6-phosphate (G-6-P) and dextran is required for activity in HSS. The average number of Ran-dependent microtubule asters per 20× magnified field after addition of 1 mg/ml of Ran(Q69L) GTP to crude extract (control), clarified HSS (C-HSS), C-HSS plus glycogen (20 mg/ml), C-HSS plus dextran (20 mg/ml), C-HSS plus dextran plus glucose-6-phosphate (5 mM). Note glucose-6-phosphate is required for microtubule assembly when nondegradable dextran is used in place of glycogen. Error bars = SD, n = 3. (B) Ran-dependent microtubule-assembly assay showing the activity of concentrated HSS. The average number of Ran-dependent microtubule asters per 20× magnified field after addition of 1 mg/ml of Ran(Q69L)GTP to crude extract (control), C-HSS (1X), and concentrated C-HSS (2X, 3X, or 4X). Average final protein concentrations (Bradford assay) of each extract are shown (in box below). Glucose-6-phosphate was added to dilution buffer in all C-HSS. Error bars = SD, n = 3. (C) Representative images of microtubule structures assembled in A. Scale bar: 3 μm. (D) Representative images of microtubule structures assembled in B. Scale bar: 3 μm. (E) Concentration of factors in C-HSS. (1) Coomassie Blue–stained PAGE of crude extract (0.5 μl), HSS (0.5 μl), and C-HSS (0.5 μl). (2) Western blot of PAGE with crude extract, HSS, C-HSS, and 4X-concentrated C-HSS (4X-C-HSS). Blots were probed with tubulin, TPX2, and XMAP215. Note the relative concentrations: crude extract is 2X as concentrated as C-HSS (1X), HSS is 3X as concentrated as C-HSS, and 4X-C-HSS is 4X as concentrated as C-HSS.
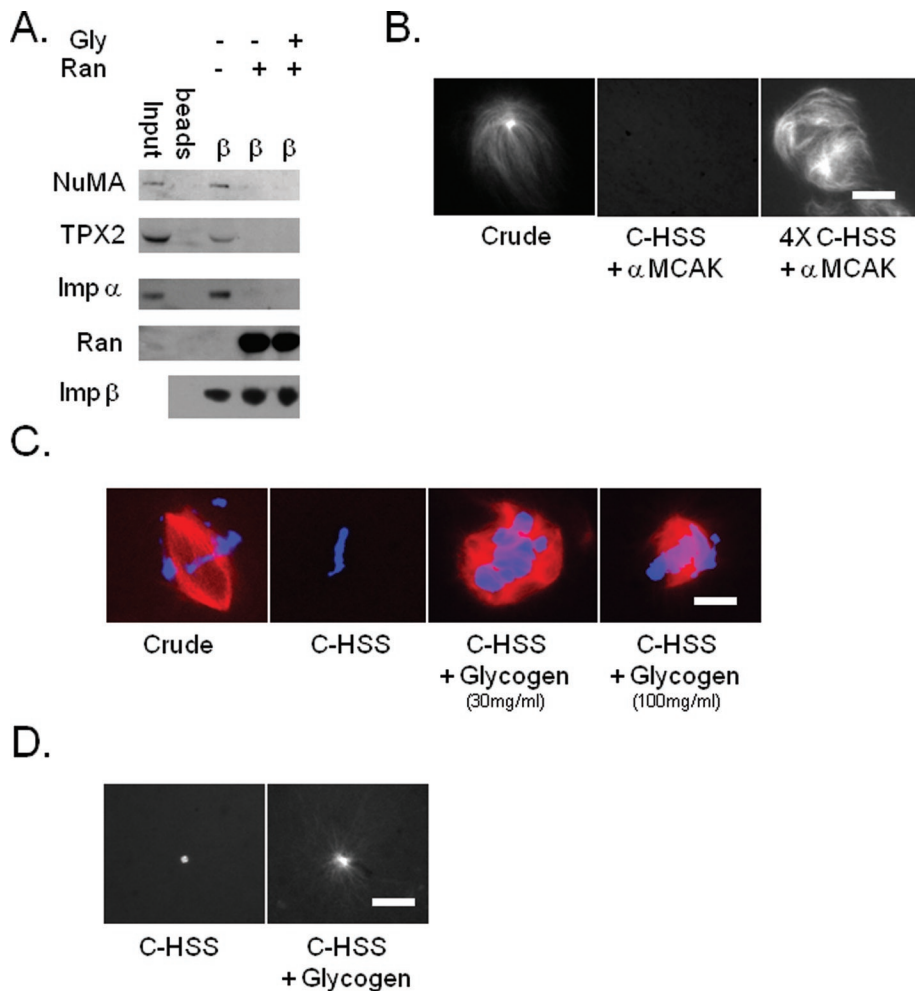
FIGURE 5: Glycogen is required for microtubule assembly. (A) Ran-dependent release of importin β cargoes does not depend on glycogen. Western blot of PAGE with C-HSS (input), Talon Dyna beads (beads) incubated in C-HSS and Talon Dyna beads bound to His-importin β incubated in C-HSS supplemented with either Ran(Q69L)GTP, Ran plus glycogen, or equal volume of buffer (CSF-XB for control). Blots were probed with antibodies for GST-RanGTP, TPX2, NuMA, importin α, and importin β. Importin β binds to TPX2, NuMA, and importin α; however, in the presence of RanGTP, importin β releases TPX2, NuMA, and importin α, and instead interacts with RanGTP. (B) MCAK antibody (300 μg/ml) induces microtubule assembly in 4X-concentrated C-HSS (4X-C-HSS; left), but not C-HSS (right). Scale bar: 3 μm. (C) The structures assembled around DNA in C-HSS plus glycogen (30 mg/ml and 100 mg/ml). Similar to Ran asters, structures appeared more bipolar at higher glycogen concentrations (100 mg/ml). No microtubule structures assemble around DNA in C-HSS without glycogen. Bipolar spindles assemble around DNA in crude extract; DNA is blue and microtubules are red. Scale bar: 10 μm. (D) Glycogen is required for microtubule assembly from *Xenopus* centrosomes in C-HSS. No microtubules assemble around centrosomes in C-HSS (left). Microtubules assemble in a radial array around centrosomes in C-HSS plus glycogen (30 mg/ml; right). Scale bar: 3 μm.

the same level as crude extract (2 APF compared with 9 APF; Figure 4B). Collectively, our data suggest that loss of microtubule assembly must be due to either dilution of multiple factors. Further experiments need to address this question.

Glycogen is also required for Ran-independent microtubule assembly

We next tested whether glycogen was required for the RanGTP-dependent release of cargoes (such as TPX2 and NuMA) from importin β. Talon Dyna beads bound to His-tagged importin β pulled down importin α and TPX2 and NuMA in C-HSS lacking glycogen (Gruss *et al.*, 2001, 2002; Nachury *et al.*, 2001). Addition of RanQ69L

eliminated this interaction (Figure 5A). These data showed that glycogen was not required to release the importin β cargoes. Thus the defect in C-HSS may be in microtubule polymerization itself.

We therefore attempted to induce microtubule assembly in HSS using physiologically relevant stimuli other than RanGTP. Addition of an inhibitory antibody to the microtubule depolymerase, MCAK (300 μg/ml), induced aster-like structures in crude extract but not HSS or C-HSS (Figure 5B; unpublished data; Desai *et al.*, 1999b; Groen *et al.*, 2009). When glycogen was added to C-HSS, MCAK antibody-induced aster assembly. The antibody also induced microtubule aster formation in 4X-HSS containing glucose-6-phosphate. These data show that microtubule assembly induced by MCAK inhibition (like RanGTP) required the metabolic and crowding activities of glycogen (Figure 5B; unpublished data).

We next tested whether glycogen is required for assembly of microtubules around sperm nuclei. This reaction is thought to be driven in part by RanGTP and in part by the Aurora B pathway (Sampath *et al.*, 2004; Kelly *et al.*, 2007; Maresca *et al.*, 2009; O'Connell *et al.*, 2009). We added sperm nuclei to C-HSS and examined for structure formation every 20 min. Assembly of microtubules around sperm nuclei in C-HSS also required glycogen (Figure 5C). As with sperm nuclei addition to crude extract, structures assembled after 60 min (Figure 5C). No structure assembled in C-HSS (Figure 5C). However, C-HSS supplemented with glycogen (30 mg/ml) restored microtubule assembly around sperm nuclei (Figure 5C). The structures assembled around sperm nuclei in crude extract were mostly bipolar spindles (>80%), as expected. Similar to Ran-induced microtubules, the types of structures in C-HSS plus glycogen depended on the concentration of glycogen. At higher glycogen concentrations (100 mg/ml), most structures were bipolar-like (~70%), and at lower concentrations (30 mg/ml), most were radial arrays (~65%; Figure 5C; unpublished data).

Finally, we tested whether glycogen was required for microtubule polymerization from isolated centrosomes in C-HSS, which is not thought to involve the Ran or Aurora B pathways. We added purified *Xenopus* centromeres to C-HSS with or without glycogen (30 mg/ml). Microtubule assembly around centrosomes also required glycogen (Figure 5D). In C-HSS, microtubules failed to assemble around centrosomes (100% did not nucleate). The centrosomes appeared as puncta (with no visible microtubules) in the presence of X-rhodamine tubulin, due to tubulin binding. With the addition of glycogen, centrosomes nucleated microtubules as radial arrays (100% nucleated; Figure 5D). Collectively, these data suggest that the defect after removal of glycogen

from C-HSS is in microtubule polymerization itself, not the Ran pathway.

Glycogen is required for spindle and centrosome aster assembly in crude mitotic extract

We used amylase treatment to determine whether glycogen was required for bipolar spindle assembly and microtubule nucleation from centrosomes in crude extracts. Amylase treatment should not disturb the glucose requirement, because glucose will still be available from the glycogen breakdown products (short glucose polymers). For spindle experiments, we used cycled spindles. Briefly, sperm nuclei were added to crude extracts, cycled through interphase by calcium addition, and then treated with amylase (1 mg/ml) or buffer control (CSF-XB) 10 min after cycling back into mitosis (with CSF addition). Spindles were allowed to assemble for 1–2 h and were then fixed and quantified. In controls, >70% of sperm nuclei initiated bipolar spindles. With amylase treatment, spindle assembly was strongly inhibited (<10% bipolar spindles; Figure 6, A and C). Addition of dextran prior to amylase treatment fully rescued bipolar spindle assembly (> 70% bipolar spindles; Figure 6, A and C). This experiment suggested that the glycogen requirement in crude extract is most likely due to molecular crowding that can be provided by a metabolically inert polymer. It also controls for possible non-specific effects of the amylase, such as protease contamination.

For centrosome experiments, purified *Xenopus* centrosomes were added to crude meiotic extracts and immediately treated with either amylase (1 mg/ml) or buffer control (CSF-XB). Centrosomes were fixed and quantified after 20 min. In controls, centrosomes nucleated microtubules in a radial array, as expected (100% nucleated; Figure 6, A and C). In amylase-treated crude extracts, centrosomes did not nucleate microtubules (100% did not nucleate; Figure 6, A and C) and appeared as puncta (with no visible microtubules) due to tubulin binding. This defect was specific to mitosis in crude extracts; nucleation of microtubules from centrosomes in interphase extract were unaffected by amylase treatment (100% nucleated microtubules; Figure 6B). Thus, glycogen may be required for the more dynamic microtubules present in mitosis (Belmont et al., 1990; Verde et al., 1992).

To better understand how glycogen affects microtubule assembly in bipolar spindles, we used real-time microscopy to image preassembled spindles treated with amylase (see Supplemental Movies 1 and 2). Assembled cycled spindles were treated with amylase (1 mg/ml) or buffer control (CSF-XB) and immediately imaged. Control spindles treated with CSF-XB buffer remained intact throughout imaging conditions. Amylase-treated spindles initially lost microtubule density (<5 min) and began to collapse after 10 min (Figure 6C). After 20 min, the microtubules (and spindle) completely disappeared (Figure 6C). These morphological changes were similar to changes observed with microtubule-depolymerizing agents, such as nocodazole (Mitchison et al., 2005), though they took longer. These data are consistent with a glycogen requirement for microtubule assembly in spindles.

DISCUSSION

Requirements for microtubule assembly in C-HSS

In this study, we prepared a clarified cytosol (C-HSS) that was active for microtubule assembly. Previous studies used HSS for microtubule polymerization assays (Parsons and Salmon, 1997), but because of the difficulty of separating HSS from membranes/glycogen, we believe the extracts used in these assays were not completely cleared of glycogen. For this reason, we used C-HSS, which more reliably removed membranes/glycogen from our extracts. This cytosol is free of membranes and ribosomes and is suitable for biochemical fractionation and, perhaps, reconstitution of spindle assembly. Microtubule-assembly activity required the following: 1) Metabolic activity that could be supplied by glycogen or glucose-6-phosphate; 2) a sufficiently high concentration of macromolecules (>60 mg/ml protein) that could be achieved by either concentrating the C-HSS or adding a macromolecular crowding agent (such as glycogen, dextran, or methyl cellulose) to more dilute C-HSS; and 3) a relatively high concentration (5–10 mM) of P_i, whose function is unclear.

Our glycogen-supplemented C-HSS system also revealed a lack of certain biochemical requirements. Small molecules in the extract, those less than the 10-kDa cutoff of the membrane used to reconcentrate the C-HSS, can be diluted 10-fold without loss of microtubule-assembly activity. ATP, GTP, glucose-6-phosphate, and P_i were not tested in this context, since they were added to the dilution buffer. Other small molecules are either not required for microtubule assembly, or are present in extract at >10-fold their required concentration. Membranes and ribosomes are also not required for Ran-dependent microtubule aster assembly. This finding is significant, in that both of these components are enriched in isolated spindles (unpublished data).

Function of glycogen

Glycogen was the particulate component removed from HSS by centrifugation that was required for Ran-dependent microtubule assembly (Figure 1). We think it unlikely that glycogen has a direct effect on microtubules. Glycogen did not localize to spindle microtubules in preliminary imaging assays (Supplemental Figure 2B), though it is difficult to assay reliably, given its high concentration in crude extract. It also did not stimulate polymerization of microtubules from pure tubulin (unpublished data), though other polymers, such as polyethylene glycol did score in this assay.

Our data point to two roles for glycogen in microtubule assembly: 1) metabolic and 2) crowding agent. In C-HSS, glycogen could be replaced by dextran and glucose-6-phosphate, but not by either alone. Dextran acts as a molecular crowding agent. Crowding agents induced more bipolar structures. At higher concentrations (>20 mg/ml) or in 4X-C-HSS (>20 mg/ml), we noticed more bipolar structures upon addition of either Ran or sperm nuclei. We believe that bipolarity, in these cases, resulted from higher levels of microtubule assembly. Further experiments need to address the correlation of level of microtubule assembly with bipolarity.

Remarkably, glycogen was also required for spindle assembly in crude extract, as evidenced by the inhibitory effect of amylase. In crude extract, glycogen depletion was rescued by dextran alone, but the short glucose polymers released by amylase in this case could presumably continue to support the metabolic role required for microtubule assembly. Thus the metabolic role and molecular crowding provided by glycogen are also required for bipolar spindle assembly.

Reducing activity and microtubule assembly

Glucose-6-phosphate (the eventual degradation product of glycogen) provides the metabolic requirement in our assays. Glucose-6-phosphate is mainly required for glycolysis (produces ATP) and the pentose phosphate pathway (produces reducing equivalents or NADPH; Van Schaftingen, 1993; Kruger and von Schaewen, 2003). Our extracts contain an ATP regeneration system (with creatine phosphate), most likely making glycolysis unnecessary for microtubule assembly. Thus we believe the reducing equivalents (NADPH) produced by the pentose phosphate pathway may constitute the metabolic requirement provided by glycogen for
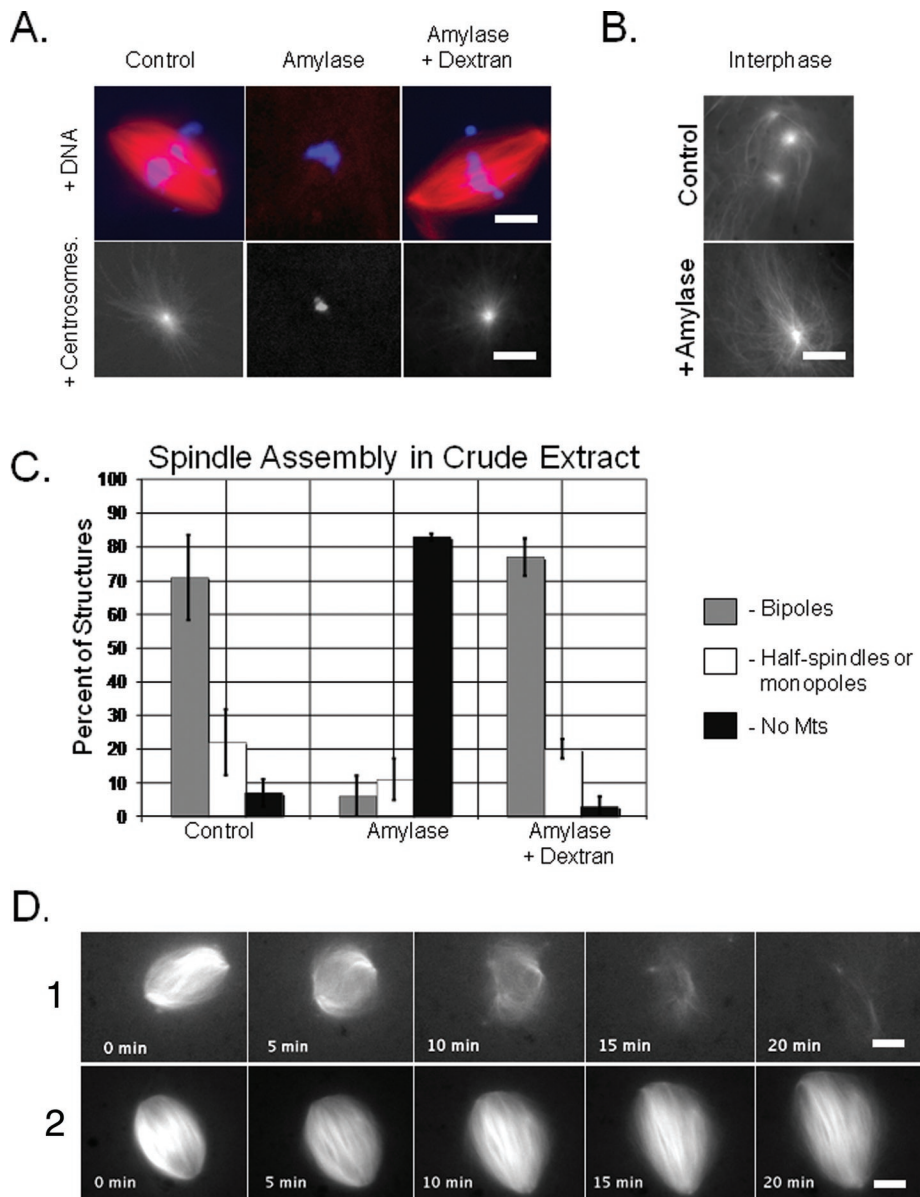
FIGURE 6: Glycogen is required for spindle and centrosome aster assembly in crude meiotic *Xenopus* extract. (A) Microtubule structures assembled around DNA (top) or centrosomes (bottom) in crude extracts treated with buffer (CSF-XB for control), amylase (1 mg/ml), or amylase (1 mg/ml) plus dextran (20 mg/ml). See (C) for quantification of spindle experiment. In control and amylase plus dextran condition, 100% of centrosomes nucleated microtubules, while 0% nucleated in amylase condition; DNA is blue and microtubules are red. Top, scale bar: 10 μm; bottom, scale bar: 3 μm. (B) Amylase treatment of interphase crude extract does not affect microtubule assembly around centrosomes. Microtubule structures assembled around centrosomes in crude extract with and without amylase (100% nucleated in both cases). Scale bar: 5 μm. (C) Spindle assembly in crude extract after amylase treatment. Average percentage of structures (bipolar spindles, half-spindles/monopoles, or no microtubules) assembled in cycled crude *Xenopus* meiotic extracts treated with buffer (CSF-XB for control), amylase (1 mg/ml), or amylase (1 mg/ml) plus dextran (20 mg/ml). Note that dextran can rescue spindle assembly defects of glycogen depletion by amylase. Error bars = SD, n = 4. (D) Images (5-min intervals) from real-time lapse imaging of cycled crude *Xenopus* meiotic extracts supplemented with X-rhodamine tubulin (50 μg/ml) and treated with buffer (CSF-XB for control) or amylase (1 mg/ml) after spindle assembly. Scale bar: 6 μm.

oxidative stress. Many cytoplasmic enzymes require electrons provided by NADPH to reduce free radicals. For example, NQO1, an NADP-dependent oxidoreductase that prevents production of radical species from one-electron reduction of quinones, was identified as influencing microtubule polymerization (Wignall *et al.*, 2004). Further experiments need to address whether oxidative damage of C-HSS is different from that of crude extract.

Tubulin also contains many cysteines, which inhibit microtubule polymerization when oxidized (Landino *et al.*, 2002). NADPH provides electrons—mainly through glutaredoxin—to reduce oxidized cysteines (Holmgren *et al.*, 2005). Therefore, without the reducing equivalents provided by NADPH, the cytosol could lack the capacity to reduce the oxidized cysteines in tubulin required for polymerization. Further experiments are required to determine whether cysteine oxidation of tubulin is more prevalent in C-HSS versus crude extract.

Activity-based fractionation of C-HSS
Biochemistry offers a nonbiased approach to identify and reconstitute the physiologically relevant activities of individual proteins and protein complexes. The reconstitution of multiple components is required to understand the full biochemistry of any one component, and the emergent properties of a multi-component system. However, unlike the actin field, which biochemically identified active complexes of proteins, such as Arp2/3 or Wave/Scar, the microtubule field has yet to identify a complex using this method (Machesky *et al.*, 1999; Blanchoin *et al.*, 2000; Gautreau *et al.*, 2004; Yang *et al.*, 2005). Single proteins that robustly modulate microtubule behavior, having activities such as bundling, severing, and depolymerizing, have been identified by biochemical fractionation (Murofushi *et al.*, 1983; Gliksman *et al.*, 1993; McNally and Vale, 1993). However, activities like nucleation and branching, which are more sensitive to dilution, are difficult to isolate and have not yet been identified using such techniques.

In this article, we identified a clarified extract (C-HSS) suitable for biochemical fractionations that contains the soluble factors required for microtubule assembly. We believe the mechanism for microtubule assembly in C-HSS is similar to that of crude extract for three reasons: 1) similar agents, such as Ran, DNA, MCAK, and centrosomes, induce polymerization; 2) similar kinetics for microtubule assembly (i.e., assembly of Ran-induced microtubule assembly occurs after ~30 min and assembly of DNA-induced microtubule structures occurs after

Ran-dependent microtubule assembly. Further experiments are required to address these questions.

What role could reducing equivalents (NADPH) play on the polymerization of microtubules? NADPH reduces damage caused by

~60 min in both extracts); and 3) glycogen is required for microtubule assembly in crude extracts. Thus our clarified extract will be useful for biochemical assays to identify physiologically relevant mechanisms for microtubule assembly.

To identify novel microtubule-assembly complexes, fractionation schemes will have to account for the metabolic requirements. For example, microtubule binding factors strongly associate with cation-exchange columns, while many of the metabolic enzymes do not. Thus the metabolic requirement would be fulfilled by combining the flow-through of a cation-exchange column with glycogen. Reconstitution of microtubule assembly could then be achieved by the addition of candidate factors to this metabolic system. Such purification schemes could be used to identify microtubule activities, such as branching factors or activators of nucleation, which have yet to be biochemically identified. Our clarified extracts will provide a powerful tool for activity-based biochemical fractionations for microtubule assembly.

MATERIALS AND METHODS
Xenopus egg extract buffers

1) CSF-XB (10 mM HEPES, pH 7.7, 100 mM KCl, 5 mM ethylene glycol tetraacetic acid [EGTA], 1 mM MgCl$_2$)
2) Extract buffer (10 mM HEPES, pH 7.7, 200 mM KCl, 1 mM dithiothreitol [DTT], 300 mM sucrose, 100 µM GTP, 100 µM MgCl$_2$)
3) Energy mix (1 mM ATP, 7.5 mM creatine phosphate, 1 mM MgCl$_2$, 100 mM sucrose)
4) Supplements-CSF-XB (S-CSF-XB; CSF-XB plus supplements: 1 mM ATP, 1 mM GTP, 1 mM DTT, 5 mM glucose-6-phosphate, 1 mM creatine phosphate)
5) CSF-XB-phosphate buffer (CSF-XB-P; CSF-XB, but using 10 mM potassium phosphate, pH 7.2, instead of 10 mM HEPES, pH 7.7)
6) S-CSF-XB-phosphate buffer or S-CSF-XB-P (CSF-XB-P plus supplements)

Xenopus egg extract purifications
Xenopus egg extract ("crude CSF extract"), which is a largely undiluted meiotic cytoplasm containing abundant organelles, was prepared as previously described (Murray, 1991; Desai et al., 1999a). Briefly, crude extracts were isolated by centrifugation of Xenopus eggs at 10,000 × g for 15 min. The cytosolic layer was collected (crude extract), and stored on ice for up to 8 h. Meiotic Xenopus HSS was prepared by supplementing CSF extract with MBP-cyclin B-Δ90 (100 µg/ml), energy mix (see Xenopus egg extract buffers) and incubated for 15 min at 20°C before centrifugation to stabilize the meiotic state of the cytoplasm (Murray and Kirschner, 1989; Murray et al., 1989). The supplemented extract was cooled to 0°C and centrifuged at 200,000 × g for 2 h in a swinging bucket rotor at 4°C (Maresca and Heald, 2006). The clear, straw-colored cytosolic layer was collected, and either used immediately for experiments or further clarification, or frozen in aliquots. HSS is clear but still contains numerous, small, low-density vesicles that may be ER-derived. Clarified HSS (C-HSS) was prepared by 10-fold dilution of HSS in S-CSF-XB-phosphate buffer, spun at 210,000 × g for 20 min in a fixed-angle rotor to remove vesicles, then concentrated back to the original volume (1X), one-half of the original volume (2X), one-third of the original volume (3X), or one-fourth of the original volume (4X) in a 10-kDa molecular-weight-cutoff Centricon Centrifugal Concentration Device (Millipore, Billerica, MA). Concentrations were determined by Bradford assay (Bio-Rad, Hercules, CA) calibrated with BSA. Both HSS and C-HSS could be stored as aliquots at −80° C without obvious change in their properties, compared with freshly prepared material. Extracts were supplemented with X-rhodamine tubulin (50 µg/ml) to visualize microtubules, as previously described (Hyman et al., 1991). Meiotic states of extracts were determined by aster assembly induced by Ran(Q69L)GTP (1 mg/ml) addition in either HSS or C-HSS supplemented with pure bovine glycogen (Sigma-Aldrich, St. Louis, MO).

Xenopus egg extract fractionations
Crude extracts (2 ml) were fractionated by centrifugation (200,000 × g, 2 h on a TLS-55, 4°C), separating the extract into four fractions: lipids (top layer), soluble cytosol (middle layer), membranes (above pellet), and yellow pellet. First, the lipid layer was carefully isolated with cutoff P200 pipette tips (approximately top 100 µl). The soluble cytosol was isolated with a syringe attached to a 0.27-gauge needle inserted a few millimeters above the membrane fraction (~600 µl isolated). The soluble cytosol was used as isolated. The membranes were isolated by resuspension in 2 ml of CSF-XB buffer, with care taken not to disturb the yellow pellet, and removed with a cutoff P1000 tip. The remaining yellow pellet (approximately 280 mg wet volume) was resuspended in 2 ml of CSF-XB.

The lipid and membrane fractions were centrifuged 20,000 × g for 20 min (tabletop microfuge, 4°C), while the yellow pellet was centrifuged at 200,000 × g for 10 min. The top 200 µl (for the lipids) and pellets (for the membranes and glycogen) were isolated and washed two more times using the same centrifugation procedure. To assay for microtubule assembly, each fraction was resuspended in S-CSF-XB equal to the original volume of crude extract (2 ml), and supplemented with 1 mg/ml Ran(Q69L)GTP. All samples were diluted in sample buffer for SDS–PAGE analysis (~100 µg loaded in each lane for each sample) and processed for Coomassie Blue staining or Western blots (Gersten et al., 1991). Blots were probed with the following antibodies: mAB414 (Abcam, Cambridge, MA), calnexin (Abcam), VDAC (Abcam), TPX2 (Groen et al., 2009), importin β (a kind gift from K. Weis, University of California, Berkeley), and γ-tubulin (Groen et al., 2004). FM4-64 (Invitrogen, Carlsbad, CA) was added to extracts at 500 µg/ml. Meiotic state of cytosol was determined by either examination of DMSO induced asters (with 10% DMSO) or Western blots probed with the mitotic specific phospho-protein antibody MPM-2 (Millipore, Billerica, MA). Western blots were quantified using ImageJ software (http://rsb.info.nih.gov/ij/download.html).

For mixing experiments, each fraction was washed one additional time with HSS (instead of CSF-XB), resuspended in HSS (equal to original volume of crude extract), supplemented with Ran(Q69L)GTP (1 mg/ml) and X-rhodamine tubulin (50 µg/ml), and imaged after 30 min. The lipid fraction was isolated from the top (instead of the pellet). For the microtubule-assembly assay, we quantified the average number of asters from 4 µl of extract appearing in 20× magnified field on five different 22 × 22 coverslips, using at least four to eight different extract preps. All images were acquired on a wide-field, upright Nikon (Tokyo, Japan) Eclipse 90i microscope using either a Nikon 60×/1.4 numerical aperture (NA) Plan-Fluor differential interference contrast (DIC) or Nikon 20×/1.4 NA Plan/APO objectives with a cooled CCD Orca ER camera (Hamamatsu, Bridgewater, NJ) driven by Metamorph (Molecular Devices, Sunnyvale, CA). HSS was never diluted more than 10X with addition of glycogen.

Purification of recombinant proteins
Constructs for GST-Ran(Q69L)GTP and MBP-cyclin B-Δ90 (a kind gift of A. Salic, Harvard Medical School, Boston, MA) were conventionally purified in bacteria. Briefly, expressed cells were lysed by sonication in lysis buffer (50 mM sodium phosphate, pH 7.7, 500 mM NaCl,

100 µM MgCl$_2$, 10% Triton [Sigma], 1 mM DTT [Sigma], 1 mM phenylmethylsulfonyl fluoride [PMSF; Sigma], plus 100 µM GTP for Ran only), using ~100 ml buffer per 1 l of bacteria. After sonication (six 30-s pulses), clarification (150,000 × *g* for 1 h), and purification by chromatography using either glutathione or amylose agarose (2 ml/l of culture) and being washed in 10 column volumes of wash buffer (lysis buffer with 10% glycerol instead of Triton), purified proteins were dialyzed overnight in extract buffer, aliquoted, and flash-frozen in liquid nitrogen for storage at −80°C.

Purification of yellow pellet and glycogen
Yellow pellet (from 2 ml of crude extract) was washed with CSF-XB (10-fold excess volume of pellet) supplemented with 10% Triton to remove membranes, RNase (1 mg/ml), and 1 mM EDTA to remove RNA (20°C for 20 min) or α-amylase (1 mg/ml) to remove glycogen. The sample was washed five times in CSF-XB by pelleting (200,000 × *g* for 10 min) and resuspending with the final wash in 2 ml of HSS (to minimize dilution). In two samples, after RNase treatment, we extracted the glycogen by phenol:chloroform (1:1) extraction and ethanol precipitation, as previously described (Hartl *et al.*, 1994). Approximately 26 mg was isolated from 1 ml of crude extract.

Meiotic spindle assembly
Cycled spindles were assembled as previously described (Desai *et al.*, 1999a). Briefly, CSF crude extract was supplemented with sperm nuclei (500 per µl) and cycled into interphase with 4 µM calcium. After 80 min, the reactions were diluted with an equal volume of CSF crude extract containing 50 µg/ml of X-rhodamine tubulin. Addition of α-amylase (1 mg/ml), CSF-XB (control), or α-amylase (1 mg/ml) and dextran (20 mg/ml) occurred 10 min after CSF add-back. One hundred structures were counted in four different extracts. Sperm nuclei (500 per µl) were added directly to C-HSS and quantified after 1 h. For real-time imaging, α-amylase (1 mg/ml) was added to cycled spindle reactions and 4 µl was placed under a 22 × 22 coverslip and immediately imaged (one image per minute) using a wide-field, upright Nikon Eclipse 90i microscope with a 20× Plan/APO NA 1.4 objective, driven by Metamorph (Molecular Devices) using an ORCA-ER (Hamamatsu). Extracts were never diluted more than 10X with addition of either dextran and/or amylase.

Microtubule pelleting assay
Ran(Q69L)GTP-treated crude extract (100 µl) or HSS (100 µl) was supplemented with either buffer (CSF-XB for control) or glycogen (20 or 200 mg/ml), incubated at room temperature for 20 min, and then pelleted in a tabletop microfuge for 20 min at 20,000 × *g*. The supernatant was removed, and the pellet was resuspended in 20 µl of sample buffer and processed for SDS–PAGE using Western blots probed with α-tubulin antibodies (Sigma) for analysis.

Directly labeled glycogen
Bovine glycogen (Sigma) was covalently labeled with X-rhodamine hydrazide (Invitrogen) after oxidation with periodic acid (Sigma). Approximately 100 mg glycogen was diluted in 1 ml of 1 mM periodic acid for 1 h at room temperature, while rotating. The oxidized glycogen was washed five times with 10 ml CSF-XB by pelleting (50,000 × *g* for 10 min) and resuspension. The sample was resuspended in 1 ml CSF-XB with 5 mM X-rhodamine hydrazide and incubated for 2 h at room temperature, while rotating. The X-rhodamine glycogen was washed five times with 10 ml CSF-XB by pelleting (50,000 × *g* for 10 min) and resuspension, and used for assays at 1–5 mg/ml for imaging.

Importin β pulldowns
Approximately 200 µl of Talon Dyna beads (Invitrogen) was incubated with 500 µl of His-importin β (1 mg/ml; purified as previously described [Mitchison *et al.*, 2004]) at 4°C, while rotating. Beads (50 µl per condition) were washed three times in CSF-XB-phosphate, and then incubated with 200 µl of C-HSS (with or without Ran and/ or glycogen) on ice for 1 h, flicking every 10 min. For controls, 50 µl Talon Dyna beads alone were incubated with C-HSS on ice for 1 h, flicking every 10 min. Samples were washed five times in S-CSF-XB and diluted in 10 µl of sample buffer for SDS–PAGE analysis and Western blots. Western blots were probed with the following antibodies: importin α (a kind gift from K. Weis), NuMa (Mitchison *et al.*, 2005), TPX2 (Groen *et al.*, 2009), and GST (for GST-Ran, a kind gift from David Miyamoto, Harvard Medical School).

Isolation of *Xenopus* centrosomes
Nuclei (3000 per µl) were added to 300 µl of fresh CSF extract and incubated for 10–20 min at room temperature. This incubation removes centrioles from nuclei. To induce interphase, 0.4 mM CaCl$_2$ was added and incubated for 1.5 h at room temperature. During this time, the DNA decondensed and the nuclei rounded up, making it easier to separate centrosomes from nuclei. Reactions were diluted at 4°C in 1.2 ml XB (10 mM HEPES, pH 7.7, 100 mM KCl, 1 mM MgCl$_2$, 100 µM CaCl$_2$) and centrifuged in a tabletop microfuge for 20 min at 5000 × *g*. Supernatant was carefully removed (i.e., everything but the harder pellet). Approximately 800 µl of XB was added to the supernatant, loaded on top of a 200 µl, 2 M sucrose cushion (in XB), and spun 20,000 × *g* for 20 min. Fractions were collected from the top. Centrosomes were very close to the 2 M sucrose cushion. Centrosomes (~30 per µl) were assayed with imaging by adding 1–2 µl of each fraction to 20 µl of CSF extract or C-HSS supplemented with X-rhodamine tubulin (50 µg/ml).

Thio-NADP absorbance
Thio-NADP (Sigma) was diluted in S-CSF-XB-P (100 mM) and added to 100 µl C-HSS extract at 1 mM, supplemented with Ran(Q69L)GTP (1 mg/ml) with or without glycogen or dextran. Absorbances at 405 nm were read on a spectrophotometer after 20 min at 23°C, as described previously (Seimiya *et al.*, 2004). The spectrophotometer was zeroed for C-HSS after immediate addition of 1 mM thio-NADP.

Electron microscopy of microtubules
Microtubules were assembled by addition of 1 mg/ml of Ran(Q69L)GTP to either crude extract or C-HSS plus 100 mg/ml glycogen. Microtubules were also assembled by addition of 10% DMSO to C-HSS. Samples were fixed in 2% formaldehyde, 0.25% glutaraldehyde in 30% glycerol/BRB-80 (80 mM PIPES, pH 6.7, 1 mM MgCl$_2$, 1 mM EGTA) for 10 min and then sedimented onto coverslips. Coverslips were then incubated in the following solutions prepared in 50 mM cacodylate buffer (pH 7.0): 25 mM lysine, 1.5% glutaraldehyde, 6 min; 1.5% glutaraldehyde, 12 min; and 1% osmium, 0.8% K-ferricyanide, 15 min, at 0°C. Samples were stained in 1% uranyl acetate for 2 h at 4°C and dehydrated by temperature reduction in an ethanol series. At 100% ethanol, coverslips were brought to room temperature and infiltrated using 2:1, 1:2 propylene oxide:epon araldite, followed by 100% epon araldite, and then mounted and polymerized at 65°C for 48 h. Spindles, selected microscopically, were remounted for sectioning at 85-nm intervals using a DMK diamond knife (kindly provided by Drukker, Cuijk, The Netherlands) on a Reichert (Depew, NY) Ultracut S microtome. Spindles were viewed and imaged on a JEOL 1200 electron microscope (Peabody, MA).

REFERENCES

Askjaer P, Galy V, Hannak E, Mattaj IW (2002). Ran GTPase cycle and importins alpha and beta are essential for spindle formation and nuclear envelope assembly in living *Caenorhabditis elegans* embryos. Mol Biol Cell 13, 4355–4370.

Belmont LD, Hyman AA, Sawin KE, Mitchison TJ (1990). Real-time visualization of cell cycle-dependent changes in microtubule dynamics in cytoplasmic extracts. Cell 62, 579–589.

Bieling P, Kandels-Lewis S, Telley IA, van Dijk J, Janke C, Surrey T (2008). CLIP-170 tracks growing microtubule ends by dynamically recognizing composite EB1/tubulin-binding sites. J Cell Biol 183, 1223–1233.

Bieling P, Laan L, Schek H, Munteanu EL, Sandblad L, Dogterom M, Brunner D, Surrey T (2007). Reconstitution of a microtubule plus-end tracking system in vitro. Nature 450, 1100–1105.

Bieling P, Telley IA, Surrey T (2010). A minimal midzone protein module controls formation and length of antiparallel microtubule overlaps. Cell 142, 420–432.

Bischoff FR, Klebe C, Kretschmer J, Wittinghofer A, Ponstingl H (1994). RanGAP1 induces GTPase activity of nuclear Ras-related Ran. Proc Natl Acad Sci USA 91, 2587–2591.

Blanchoin L, Amann KJ, Higgs HN, Marchand JB, Kaiser DA, Pollard TD (2000). Direct observation of dendritic actin filament networks nucleated by Arp2/3 complex and WASP/Scar proteins. Nature 404, 1007–1011.

Bolte S, Talbot C, Boutte Y, Catrice O, Read ND, Satiat-Jeunemaitre B (2004). FM-dyes as experimental probes for dissecting vesicle trafficking in living plant cells. J Microsc 214, 159–173.

Buendia B, Antony C, Verde F, Bornens M, Karsenti E (1990). A centrosomal antigen localized on intermediate filaments and mitotic spindle poles. J Cell Sci 97, 259–271.

Carazo-Salas RE, Guarguaglini G, Gruss OJ, Segref A, Karsenti E, Mattaj IW (1999). Generation of GTP-bound Ran by RCC1 is required for chromatin-induced mitotic spindle formation. Nature 400, 178–181.

Casanova CM, Rybina S, Yokoyama H, Karsenti Mattaj IW (2008). Hepatoma up-regulated protein is required for chromatin-induced microtubule assembly independently of TPX2. Mol Biol Cell 11, 4900–4908.

Chang P, Jacobson MK, Mitchison TJ (2004). Poly(ADP-ribose) is required for spindle assembly and structure. Nature 432, 645–649.

Davis FM, Tsao TY, Fowler SK, Rao PN (1983). Monoclonal antibodies to mitotic cells. Proc Natl Acad Sci USA 80, 2926–2930.

Desai A, Deacon HW, Walczak CE, Mitchison TJ (1997). A method that allows the assembly of kinetochore components onto chromosomes condensed in clarified *Xenopus* egg extracts. Proc Natl Acad Sci USA 94, 12378–12383.

Desai A, Murray A, Mitchison TJ, Walczak CE (1999a). The use of *Xenopus* egg extracts to study mitotic spindle assembly and function *in vitro*. Methods Cell Biol 61, 385–412.

Desai A, Verma S, Mitchison TJ, Walczak CE (1999b). Kin I kinesins are microtubule-destabilizing enzymes. Cell 96, 69–78.

Gautreau A, Ho HY, Li J, Steen H, Gygi SP, Kirschner MW (2004). Purification and architecture of the ubiquitous Wave complex. Proc Natl Acad Sci USA 101, 4379–4383.

Gersten DM, Kimball H, Bijwaard KE (1991). Gel electrophoresis in the presence of soluble, aqueous polymers: horizontal sodium dodecyl sulfate-polyacrylamide gels. Anal Biochem 197, 59–64.

Gliksman NR, Parsons SF, Salmon ED (1993). Cytoplasmic extracts from the eggs of sea urchins and clams for the study of microtubule-associated motility and bundling. Methods Cell Biol 39, 237–251.

Golshani-Hebroni SG, Bessman SP (1997). Hexokinase binding to mitochondria: a basis for proliferative energy metabolism. J Bioenerg Biomembr 29, 331–338.

Groen AC, Cameron LA, Coughlin M, Miyamoto DT, Mitchison TJ, Ohi R (2004). XRHAMM functions in Ran-dependent microtubule nucleation and pole formation during anastral spindle assembly. Curr Biol 14, 1801–1811.

Groen AC, Maresca TJ, Gatlin JC, Salmon ED, Mitchison TJ (2009). Functional overlap of microtubule assembly factors in chromatin-promoted spindle assembly. Mol Biol Cell 20, 2766–2773.

Gruss OJ, Carazo-Salas RE, Schatz CA, Guarguaglini G, Kast J, Wilm M, Le Bot N, Vernos I, Karsenti E, Mattaj IW (2001). Ran induces spindle assembly by reversing the inhibitory effect of importin alpha on TPX2 activity. Cell 104, 83–93.

Gruss OJ, Wittmann M, Yokoyama H, Pepperkok R, Kufer T, Sillje H, Karsenti E, Mattaj IW, Vernos I (2002). Chromosome-induced microtubule assembly mediated by TPX2 is required for spindle formation in HeLa cells. Nat Cell Biol 4, 871–879.

Hartl P, Olson E, Dang T, Forbes DJ (1994). Nuclear assembly with lambda DNA in fractionated Xenopus egg extracts: an unexpected role for glycogen in formation of a higher order chromatin intermediate. J Cell Biol 124, 235–248.

Holmgren A, Johansson C, Berndt C, Lonn ME, Hudemann C, Lillig CH (2005). Thiol redox control via thioredoxin and glutaredoxin systems. Biochem Soc Trans 33, 1375–1377.

Hyman A, Drechsel D, Kellogg D, Salser S, Sawin K, Steffen P, Wordeman L, Mitchison T (1991). Preparation of modified tubulins. Methods Enzymol 196, 478–485.

Kalab P, Weis K, Heald R (2002). Visualization of a Ran-GTP gradient in interphase and mitotic *Xenopus* egg extracts. Science 295, 2452–2456.

Kelly AE, Sampath SC, Maniar TA, Woo EM, Chait BT, Funabiki H (2007). Chromosomal enrichment and activation of the Aurora B pathway are coupled to spatially regulate spindle assembly. Dev Cell 12, 31–43.

Kinoshita K, Arnal I, Desai A, Drechsel DN, Hyman AA (2001). Reconstitution of physiological microtubule dynamics using purified components. Science 294, 1340–1343.

Klebe C, Bischoff FR, Ponstingl H, Wittinghofer A (1995). Interaction of the nuclear GTP-binding protein Ran with its regulatory proteins RCC1 and RanGAP1. Biochemistry 34, 639–647.

Koffa MD, Casanova CM, Santarella R, Kocher T, Wilm M, Mattaj IW (2006). HURP is part of a Ran-dependent complex involved in spindle formation. Curr Biol 16, 743–754.

Kruger NJ, von Schaewen A (2003). The oxidative pentose phosphate pathway: structure and organisation. Curr Opin Plant Biol 6, 236–246.

Landino LM, Hasan R, McGaw A, Cooley S, Smith AW, Masselam K, Kim G (2002). Peroxynitrite oxidation of tubulin sulfhydryls inhibits microtubule polymerization. Arch Biochem Biophys 398, 213–220.

Lourim D, Krohne G (1998). Chromatin binding and polymerization of the endogenous Xenopus egg lamins: the opposing effects of glycogen and ATP. J Cell Sci 111, 3675–3686.

Machesky LM, Mullins RD, Higgs HN, Kaiser DA, Blanchoin L, May RC, Hall ME, Pollard TD (1999). Scar, a WASp-related protein, activates nucleation of actin filaments by the Arp2/3 complex. Proc Natl Acad Sci USA 96, 3739–3744.

Maresca TJ, Groen AC, Gatlin JC, Ohi R, Mitchison TJ, Salmon ED (2009). Spindle assembly in the absence of a RanGTP gradient requires localized CPC activity. Curr Biol 19, 1210–1215.

Maresca TJ, Heald R (2006). Methods for studying spindle assembly and chromosome condensation in *Xenopus* egg extracts. Methods Mol Biol 322, 459–474.

McNally FJ, Vale RD (1993). Identification of katanin, an ATPase that severs and disassembles stable microtubules. Cell 75, 419–429.

Mitchison TJ, Maddox P, Gaetz J, Groen A, Shirasu M, Desai A, Salmon ED, Kapoor TM (2005). Roles of polymerization dynamics, opposed motors, and a tensile element in governing the length of *Xenopus* extract meiotic spindles. Mol Biol Cell 16, 3064–3076.

Mitchison TJ, Maddox P, Groen A, Cameron L, Perlman Z, Ohi R, Desai A, Salmon ED, Kapoor TM (2004). Bipolarization and poleward flux correlate during *Xenopus* extract spindle assembly. Mol Biol Cell 15, 5603–5615.

Moses RM, Masui Y (1989). Cytostatic factor (CSF) in the eggs of *Xenopus laevis*. Exp Cell Res 185, 271–276.

Moses RM, Masui Y (1990). Cytostatic factor (CSF) activity in cytosols extracted from *Xenopus laevis* eggs. Exp Cell Res 186, 66–73.

Murofushi H, Minami Y, Matsumoto G, Sakai H (1983). Bundling of microtubules *in vitro* by a high molecular weight protein prepared from the squid axon. J Biochem 93, 639–650.

Murray AW (1991). Cell cycle extracts. Methods Cell Biol 36, 581–605.

Murray AW, Kirschner MW (1989). Cyclin synthesis drives the early embryonic cell cycle. Nature 339, 275–280.

Murray AW, Solomon MJ, Kirschner MW (1989). The role of cyclin synthesis and degradation in the control of maturation promoting factor activity. Nature 339, 280–286.

Nachury MV, Maresca TJ, Salmon WC, Waterman-Storer CM, Heald R, Weis K (2001). Importin beta is a mitotic target of the small GTPase Ran in spindle assembly. Cell 104, 95–106.

Niethammer P, Kueh HY, Mitchison TJ (2008). Spatial patterning of metabolism by mitochondria, oxygen, and energy sinks in a model cytoplasm. Curr Biol 18, 586–591.

O'Connell CB, Loncarek J, Kalab P, Khodjakov A (2009). Relative contributions of chromatin and kinetochores to mitotic spindle assembly. J Cell Biol 187, 43–51.

Parsons SF, Salmon ED (1997). Microtubule assembly in clarified *Xenopus* egg extracts. Cell Motil Cytoskeleton 36, 1–11.

Popov AV, Pozniakovsky A, Arnal I, Antony C, Ashford AJ, Kinoshita K, Tournebize R, Hyman AA, Karsenti E (2001). XMAP215 regulates microtubule dynamics through two distinct domains. EMBO J 20, 397–410.

Roach PJ (2002). Glycogen and its metabolism. Curr Mol Med 2, 101–120.

Sampath SC, Ohi R, Leismann O, Salic A, Pozniakovski A, Funabiki H (2004). The chromosomal passenger complex is required for chromatin-induced microtubule stabilization and spindle assembly. Cell 118, 187–202.

Sawin KE, LeGuellec K, Philippe M, Mitchison TJ (1992). Mitotic spindle organization by a plus-end-directed microtubule motor. Nature 359, 540–543.

Seimiya M, Osawa S, Hisae N, Shishido T, Yamaguchi T, Nomura F (2004). A sensitive enzymatic assay for the determination of sucrose in serum and urine. Clin Chim Acta 343, 195–199.

Tsai MY, Wiese C, Cao K, Martin O, Donovan P, Ruderman J, Prigent C, Zheng Y (2003). A Ran signalling pathway mediated by the mitotic kinase Aurora A in spindle assembly. Nat Cell Biol 5, 242–248.

Vagnarelli P, Earnshaw WC (2004). Chromosomal passengers: the four-dimensional regulation of mitotic events. Chromosoma 113, 211–222.

Van Schaftingen E (1993). Glycolysis revisited. Diabetologia 36, 581–588.

Verde F, Berrez JM, Antony C, Karsenti E (1991). Taxol-induced microtubule asters in mitotic extracts of *Xenopus* eggs: requirement for phosphorylated factors and cytoplasmic dynein. J Cell Biol 112, 1177–1187.

Verde F, Dogterom M, Stelzer E, Karsenti E, Leibler S (1992). Control of microtubule dynamics and length by cyclin A- and cyclin B-dependent kinases in *Xenopus* egg extracts. J Cell Biol 118, 1097–1108.

Wignall SM, Gray NS, Chang YT, Juarez L, Jacob R, Burlingame A, Schultz PG, Heald R (2004). Identification of a novel protein regulating microtubule stability through a chemical approach. Chem Biol 11, 135–146.

Wilde A, Lizarraga SB, Zhang L, Wiese C, Gliksman NR, Walczak CE, Zheng Y (2001). Ran stimulates spindle assembly by altering microtubule dynamics and the balance of motor activities. Nat Cell Biol 3, 221–227.

Wittmann T, Wilm M, Karsenti E, Vernos I (2000). TPX2, a novel *Xenopus* MAP involved in spindle pole organization. J Cell Biol 149, 1405–1418.

Yang CP, Chen MS, Liaw GJ, Chen SF, Chou G, Fan SS (2005). Using *Drosophila* eye as a model system to characterize the function of *mars* gene in cell-cycle regulation. Exp Cell Res 307, 183–193.

Zheng Y, Tsai MY (2006). The mitotic spindle matrix: a fibro-membranous lamin connection. Cell Cycle 5, 2345–2347.

Zimmerman SB, Minton AP (1993). Macromolecular crowding: biochemical, biophysical, and physiological consequences. Annu Rev Biophys Biomol Struct 22, 27–65.